Unified multifractal atmospheric dynamics tested in the tropics: part II, vertical scaling and generalized scale invariance

A. Lazarev, D Schertzer, S. Lovejoy, Y. Chigirinskaya

Nonlinear Processes in Geophysics (1994) 1: 115 - 123

Nonlinear Processes in Geophysics

Unified multifractal atmospheric dynamics tested in the tropics: part II, vertical scaling and generalized scale invariance

A. Lazarev[1], D. Schertzer[2], S. Lovejoy[2*] and Y. Chigirinskaya[2**]

[1] Space Research Institute, Profsoyuznaya pl., 84/32, 117810 Moscow, Russia
[2] Laboratoire de Météorologie Dynamique, Université Pierre et Marie Curie, 4 Place Jussieu, 75252 Paris Cedex 05, France
[*] on leave from the Physics Dept., McGill Univ., Canada / [**]on leave from Math. and Mech. Dept., Moscow Univ., Russia

Received 21 December 1993 - Accepted 28 March 1994 - Communicated by S.S. Moiseev

Abstract. We empirically investigate the scaling behaviour of the horizontal wind along the vertical direction using 287 radiosonde soundings with a resolution of 50 m. We compare the results obtained with those of the horizontal temporal behaviour in the framework of Generalized Scaling Invariance and the Unified Scaling model of atmospheric dynamics. We find the scaling to be very well respected over the range 50 m - 13 km (nearly the entire troposphere) and we estimate the universal multifractal indices which characterize the statistics in the vertical. By comparing our results with those obtained in the horizontal we show that the degree of stratification is different for mean and extreme structures. Finally, we theoretically discuss the necessary improvements to the Unified Multifractal model needed to account for them.

1 Introduction

Although mesoscale fluctuations of the wind field in the atmosphere have been observed for many years, there is no consensus as to their statistical description. This is especially true in the case of the tropical atmosphere which possesses a high degree of intermittency associated with buoyancy driven convection, and a tendency towards self-organization of small-scale convective cells into large-scale coherent structures such as tropical cyclones. In this part, we discuss further the relevance of the Unified Scaling model of atmospheric dynamics (Schertzer and Lovejoy 1983, 1985; Lovejoy et al., 1993) by considering the scaling properties of turbulent wind fluctuations in tropical atmosphere *along the vertical.* After recalling the motivations and basic ingredients of Generalized Scale Invariance necessary to account the scaling anisotropy, we estimate the universal exponents of the wind shears along the vertical. With the help of these results, as well as the analogous ones found in the horizontal (presented in part I, Chigirinskaya et al., 1994), we show how these anisotropic scaling properties give direct support to the Unified Scaling model of atmospheric dynamics while contradicting the classical model which involves isotropic two dimensional and isotropic three dimensional turbulence separated by a "meso-scale gap" or "dimensional transition" (Schertzer and Lovejoy, 1985).

Indeed, in order to take into account the dominant role of buoyancy forces it was hypothesized, partially following the arguments of the classical "buoyancy sub-range" (Bolgiano, 1959; Obukhov, 1959), that the buoyancy force variance flux (ϕ) should play the same role as (ε) in classical 3-D turbulence (Kolmogorov, 1941; Obukhov, 1941) but only along the vertical, contrary to the classical "buoyancy sub-range" which hypothesizes an isotropic turbulence. The different horizontal and vertical scaling regimes found here correspond to two coupled sets of scaling equations for respectively the horizontal shears $\Delta v(\Delta x) = |\underline{v}(\underline{x}+\underline{u}\Delta x)-\underline{v}(\underline{x})|$ isotropically distributed over the different horizontal (unitary) direction $\underline{u}$ and vertical shears of the horizontal wind $\Delta v(\Delta z) = |\underline{v}(\underline{z}+\underline{k}\Delta z)-\underline{v}(\underline{z})|$, $\underline{k}$ being the unit vector of the vertical axis:

$$\Delta v(\Delta x) \overset{d}{=} \left(\varepsilon(\Delta x)\right)^{a_h} \Delta x^{H_h} \quad (1)$$

$$\Delta v(\Delta z) \overset{d}{=} (\phi(\Delta z))^{a_v} \Delta z^{H_v} \quad (2)$$

($\overset{d}{=}$ means equality in probability distributions) with a_h=1/3, H_h=1/3, a_v=1/5, H_v=3/5. These exponents are obtained with purely dimensional arguments (the horizontal - Kolmogorov, 1941; Obukhov, 1941; and the vertical - Bolgiano, 1959; Obukhov, 1959). Contrary to the original derivations, the intermittent scaling fluctuations of both ε and ϕ are not neglected since their scale dependency is explicit and furthermore we will demonstrate that this implies that ϕ and ε (see part I) both display Self Organized Critical behaviour. In contrast to the original derivation involving two isotropic regimes, each characterized by a

Correspondence to: D. Schertzer

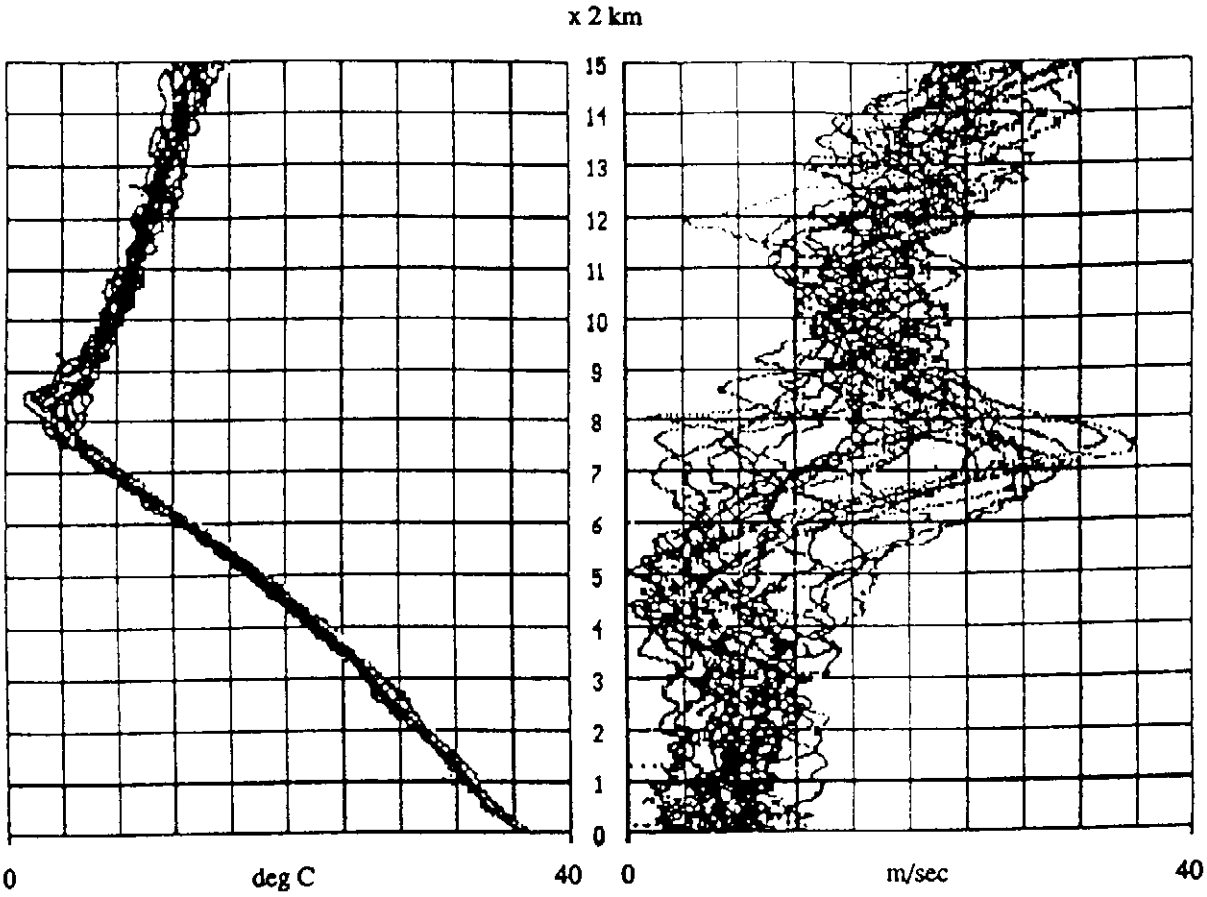

Fig. 1. A representative sequence of temperature (left panel) and horizontal wind speed (right panel) profiles vs. height.

different exponent and separated from each other by a break in the scaling, the unified scaling model results in considering a single scaling but anisotropic regime (over all meteorogically significant scales). Rather than first postulating isotropy, and only secondly scaling (with the implication of a meso-scale break), we only postulate scaling, while expecting it to be anisotropic at all scales.

The interpretation of Eqs. (1, 2) is that we have:

$$\varepsilon(\Delta x)^{\frac{1}{3}} \approx \phi(\Delta z)^{\frac{1}{5}} \text{ when } \Delta x^{\frac{1}{3}} \approx \Delta z^{\frac{3}{5}} \tag{3}$$

where Δx, and Δz are the horizontal and vertical extents of an eddy, and ε, ϕ are the corresponding kinetic energy and buoyancy force variance fluxes respectively.

This corresponds to a scalar, but highly nonlinear, balance between these two fluxes. An immediate consequence is that iso-shear surfaces may be ellipsoids rather than spheres, corresponding to the simplest case of Generalized Scale Invariance: self affine (multi-) fractal fields. More precisely, in the self affine systems the corresponding generator (G) of scale transformations ($T\lambda$) corresponds to a diagonal matrix instead of the identity (of isotropic scaling):

$$T_\lambda = \lambda^{-G} = e^{-G\log\lambda} \quad G = \begin{pmatrix} 1 & 0 & 0 \\ 0 & 1 & 0 \\ 0 & 0 & H_z \end{pmatrix} \tag{4}$$

$$\Delta \underline{v}(T_\lambda \Delta \underline{x}) \overset{d}{=} \lambda^{-H_h} \Delta \underline{v}(\Delta \underline{x}) \tag{5}$$

with $H_z = H_h/H_v = 5/9$. The trace of G is the (effective) "elliptical dimension" of the space, i.e. $D_{el} = 2 + H_z = 23/9 = 2.555...$ for this self-affine stratified turbulence (Schertzer and Lovejoy, 1983, 1985). It characterizes how the volumes of eddies change with scale.

A convenient reference scale, called the "sphero-scale"[3] (Schertzer and Lovejoy, 1983, 1985) will exist where the horizontal and vertical extents of an eddy will be equal: $\Delta x_s = \Delta z_s$. This scale is not at all a characteristic scale. At scales smaller than Δx_s, and assuming $H_h < H_v$ (the relevant case) the eddies will be all vertically elongated, resembling convective cells, whereas for scales larger than Δx_s, they are all flattened in the horizontal, becoming more and more horizontally stratified at larger and larger scales.

[3] The corresponding scale need not in fact be isotropic (i.e. spherical), this is only the simplest case.

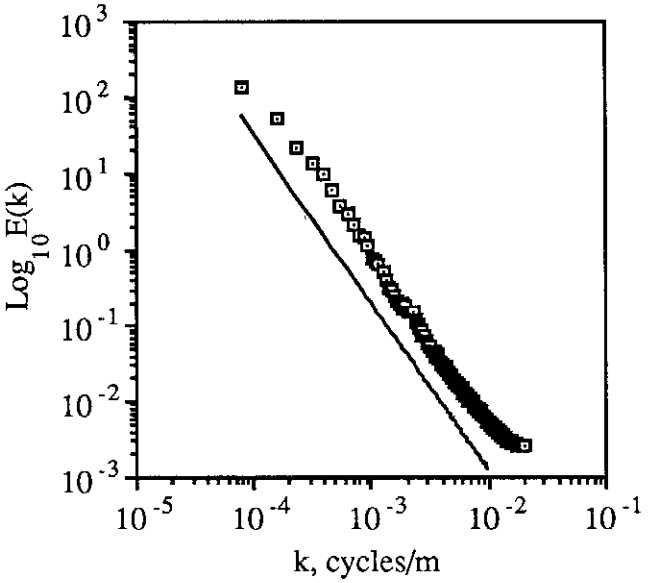

Fig. 2. The mean spectrum of 287 radiosondes at 50 m resolution, over a total depth of 13.3 km. The straight line is for reference with slope -2.2 .

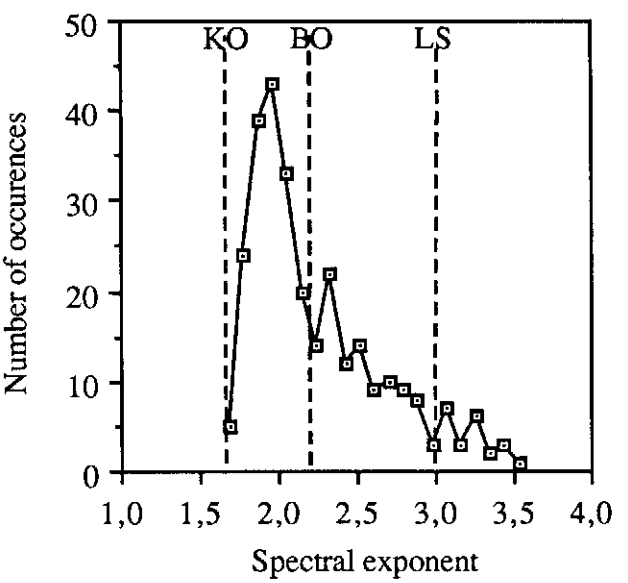

Fig. 3. The distribution of spectral exponents for individual spectra. Dashed lines correspond to Kolmogorov-Obukhov (KO) -5/3 , Bolgiano-Obukhov (BO) -11/5, and Lumley-Shur (LS) -3 laws, respectively. Clearly, the values 5/3 and 3 are rarely encountered.

2 Initial Data and Pre-Processing

Vertical wind speed profiles have been measured using radiosondes during two expeditions of a research ship to a tropical part of the Pacific Ocean. The total experimental area was between latitudes 2°N - 29°N and longitudes 106°E - 153°E (most of the soundings were between latitudes 2°N - 20°N and longitudes 125°E - 140°E). The entire set of balloon data (horizontal wind V, temperature T, relative humidity Q) consists of 187 vertical profiles for the year 1989 (May - August) and 138 profiles for the year 1990 (July - October). All atmospheric variables were measured along the balloon rise paths, which for simplicity of interpretation, were considered vertical. The time difference between the beginning and the end of each balloon flight is neglected.

The vertical resolution of the balloon sensors was about 20-25 m (data were transmitted every 5 sec of balloon flight). The data were first interpolated onto regularly spaced intervals with vertical resolution of 25 m, and then averaged over 50 m layers from near the surface to approximately 30 - 35 km. Averaging over 50 m layers excludes most of the motions associated with the particular balloon aerodynamics as well as false wind velocity maxima/minima and of course, the effects of any atmospheric eddies lesser than 50m. Fig. 1 displays the detailed structure of the flow in the atmosphere with the help of a representative sequence of these profiles for horizontal wind speed and temperature vs. height.

Due to peculiarities of the radar tracking operation, the minimum height varied from 150 to 450 m. This yields a lower cut-off of data - we chose a minimum height for analysis of 500 m. This minimum altitude does not cause any loss of generality, at worst it could be understood as a rejection of the atmospheric surface layer with possibly different statistics[4]. In this study we shall analyze only turbulent wind data in the troposphere. Data of the turbulent temperature profile and those from the stratosphere will be discussed elsewhere. Thus, the upper height cut-off was chosen somewhere near the tropopause (see Fig. 1) which in our framework corresponds to a peak of variability. Indeed, near the tropopause, many balloons burst, and sensors failed. Occasionally strong downdraughts or horizontal jet streams were present; but if the balloons managed to pass through - then they were able to reach much higher altitudes. To eliminate these effects on our statistics we fixed the upper cut-off at the height 13300 m. Following these pre-processing procedures, the total data base was reduced to 287 individual profiles (167 for 1989 and 120 for 1990), which were used in the analysis described below.

[4]Actually, unlike most theories which only apply under rather special conditions (i.e. not too stable, not too unstable), our results apparently apply under all conditions; only the amplitude of the fluctuations is a function of altitude and meteorology (see also Schertzer and Lovejoy (1985) for a discussion of the effect of varying altitude and meteorological conditions). Nevertheless, it would be interesting and important to test it much closer to the surface.

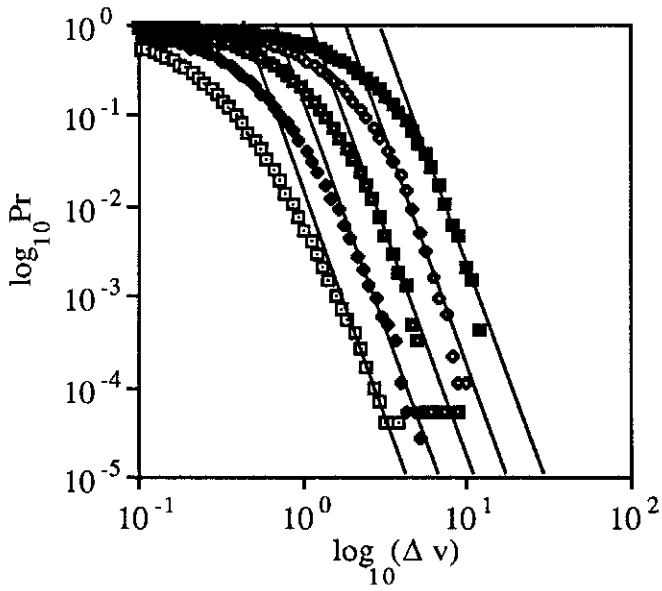

Fig. 4. Probability distributions for layers of thickness varying from 50 m to 800 m (vertical separation between curves increases from left to right by factor of 2) with straight lines with H_v=0.51 $q_{D,v}$=5 for comparison.

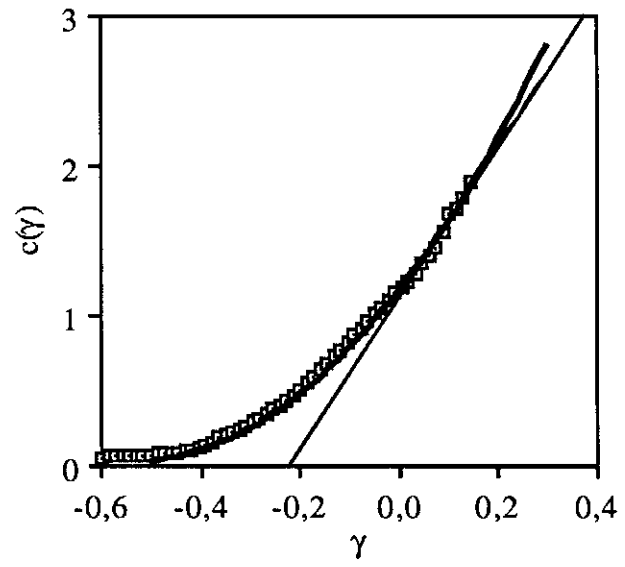

Fig. 5. $c(\gamma)$ function calculated from the probability distribution for 50 m thick layers (points) compared to the theoretical bare and dressed $c(\gamma)$ calculated with the parameters $C_{1,v}$=0.09, α=1.85, H_v=0.5, q_D=5.

3 Spectrum of Wind Fluctuations

The energy spectrum $E(k)$ averaged over 287 individual wind profiles (Fig. 2) possesses a long (over 2 orders of magnitude) power law scaling region of the form $E(k) = k^{-\beta_v}$ in the wavelength interval from 80 m to 12.5 km with exponent $\beta_v \approx 2.20$. This is in excellent agreement with Bolgiano-Obukhov (BO) spectrum for convection in a stably stratified atmosphere (Bolgiano, 1959; Obukhov, 1959) which gives β_v=11/5 (see also, Brandenberg, 1992; Yakhot, 1992). Still it appears that this agreement is for the average spectrum, individual spectra show some variability of the estimated slopes from ≈ 5/3 to 3.5 (see Fig. 3). This variability can also be seen in the results of other investigators, who report various spectral exponents. In a unified multifractal framework, the spectral exponents of individual realizations are poorly defined and regressions will yield random variables with large variability.

The first test of the BO spectrum was, Endlich et al. (1969) who determined power spectral densities from vertical soundings of horizontal winds that were measured by means of radar-tracked "Jimspheres" obtaining[5] exponents of roughly 5/2. Rosenberg et al. (1974) using NASA vertical smoke trail measurements found a value of about[6] 2.75. Finally, Daniels (1982) reported values[7] of about 2.5.

The spectral exponent β_v is related to the real space scaling exponent H_v (see Eq.(2)) by:

$$\beta_v = 1 + 2H_v - K(2/3) \quad (6)$$

Ignoring first the small multifractal intermittency corrections ($-K(2/3)$), from our theoretical estimate of H_v=3/5, we obtain β_v =11/5. The estimate of H_v is also very close to values first reported by Adelfang (1971) (who found a value of 0.60 on the basis of thousands of "Jimsphere" flights and structure functions), and to the value 0.6 obtained by Schertzer and Lovejoy (1983, 1985) using data with a 50 m spatial resolution at 3-hour intervals in Landes (France) and probability distributions.

There are however two main and closely related differences of this scaling with that of the classical "buoyancy subrange". The first is the very large range of scales over which it holds; indeed, the scaling interval is over virtually the entire range of meteorologically significant vertical scales. The ability of a single measurement device to cover the entire range in this way is a significant advantage of studying the vertical rather than the horizontal direction. In the latter case many different measuring campaigns and devices are necessary (for discussion and review, see Schertzer and Lovejoy, 1985 and Lovejoy et al., 1993).

[5]These measurements were in the 200 m to 16 km altitude region, and over the wavelength range of 100 m to 5 km. There was some dispersion of the individual spectral slopes although the authors concluded that the values were never as low as 5/3.

[6]In the altitude range 5 - 18 km and in the wavelength range 100 m to 3.6 km.

[7]With a total of 1200 vertical profile measurements made with rawinsondes in the 4 - 16 km altitude range for wavelengths in between 80 m - 4 km.

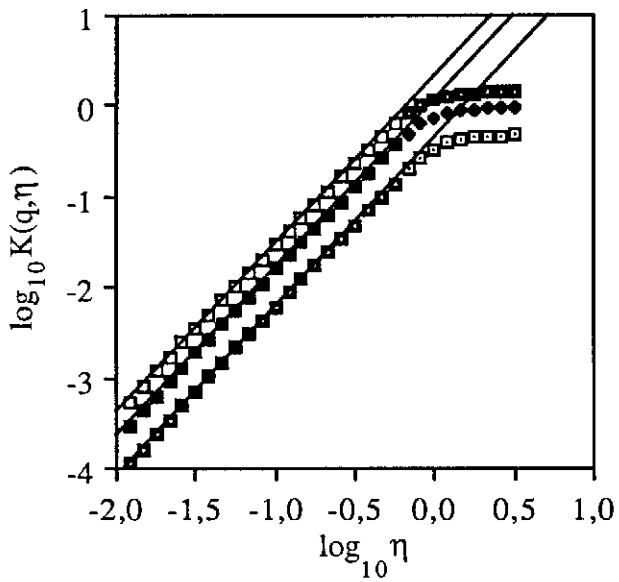

Fig. 6. Results of the DTM analysis with q=2.5, 2, 1.5 , top to bottom, respectively, the straight lines correspond to α= 1.85.

The second difference is that contrary to the BO theory, the scaling found here does not correspond isotropic scaling, since as evidenced in Part I the corresponding horizontal spectrum is quite different. The latter was obtained from data belonging to similar "Typhon" experiments in the same area and during the same period, but collected along the horizontal with the help of instrumented aircraft. The corresponding horizontal exponent was estimated to be $\beta_h \approx 5/3$ (and hence $H_h \approx 1/3$) as predicted by Kolmogorov (1941) and Obukhov (1941). Indeed, as technology has improved, and the size of wind data bases has increased, it has become quite clear that the horizontal scaling with exponent $\approx 5/3$ continues up to at least several hundred kilometers - right through the mesoscale (Nastrom and Gage, 1983; Lilly, 1983). However, perhaps the most convincing evidence to date for horizontal scaling comes not directly from velocity data at all, but rather from satellite imagery of clouds which show remarkably good scaling over a wide range of wavelengths and length scales spanning at least 300 m to 4000 km (Lovejoy et al., 1993). The radiances associated with the latter are nonlinearly coupled with the velocity field and the dynamical scaling is expected to reflect itself in the former. Conversely, it can be argued that a break in the scaling of the velocity field associated with a meso-scale gap and with a "dimensional transition" from small scale three dimensional to large scale two dimensional turbulence would be particularly obvious in the cloud and radiance fields[8].

[8]Whereas the (vector) wind field has two quadratic invariants in 2-D turbulence (the enstrophy and the energy fluxes), and hence two not very different scaling regimes, this is not true of the corresponding passive scalars; the latter will display a very drastic break at the transition from enstrophy to energy flux dominated cascades.

The ubiquity of scaling with $\beta_v \approx 11/5$ in the vertical and $\beta_h \approx 5/3$ in the horizontal corresponds to the unique anisotropic but scaling regime of atmospheric dynamics as postulated in the Unified Scaling model of atmospheric dynamics and recalled in the section 1. There is no evidence for either isotropic three dimensional nor for isotropic two dimensional turbulence, the atmosphere appears to be anisotropic but scaling throughout. It should perhaps be recalled that such anisotropic scaling implies that the atmosphere is progressively more and more stratified at larger and larger scales. The frequently quoted scale height of the decrease in the mean pressure is apparently not visible in the dynamically significant vertical fluctuations.

We may finally make some comments on the conventional explanation for the realization to realization variability of the spectrum. The cause of this variability is usually attributed to the stratification conditions. Since it is evident that if locally isotropic turbulence (Kolmogorov - Obukhov (KO)) can ever be realized in the atmosphere it will only be under neutral stratification (motions over each direction must have equal probability). Some investigations have been carried out during changes of atmospheric stratification to investigate this. Thus, Myrup (1969) analyzed data of research plane horizontal flights on several heights during the morning heating of the atmosphere and during the change of stratification from stable to neutral. He found that for stable stratification (both for horizontal and vertical sections of turbulent wind field) spectra possess slopes from 11/5 to 3, but for the case of neutral stratification spectra were closer to the KO theory.

From the point of view of the Unified Scaling model, the problem is that the notion of stable or unstable stratification is scale dependent. For example, Schertzer and Lovejoy (1985) showed that if the Richardson number is defined as a function of the thickness of a layer, that it was scaling with exponent = 1. This means that any sufficiently thick layer would be stable while nonetheless containing many thin unstable layers (in a scaling hierarchy). The qualification "stable " or "unstable" is therefore a scale dependent concept, and experiments which are "filtered" so as to only consider one type of situation or another will involve complex scale dependent conditioning. The fact this conditioning - based on subjective scale dependent large scale criterion - is more or less equivalent to a classificaion of the data according to their spectra is not surprising.

4 Probability distribution function of wind shear

In Part I, we discussed the notion of Self Organized Criticality in the context of stochastic multifractals, as

Table 1. Comparison of universal multifractal indices (including the dressing dimension D) for *kinetic energy flux* in the atmosphere in the vertical, horizontal and time.

Variable	Vertical (this paper)	Horizontal (part I)	Time (Schmitt et al., 1993)
α	1.85±0.05	1.35±0.07	1.50±0.05
C_1	0.59±0.05	0.30±0.05	0.25±0.05
q_D +	1.7±0.1	2.4±0.05	2.5±0.3
$\gamma_{D,s}$ *	1.28±0.05	0.70±0.05	0.60±0.05
$\gamma_{d,s}(D_s=0)$ #	0.94±0.05	0.72±0.05	0.68±0.05
$\gamma_{d,s}(D_s=0.5)$ #	1.26±0.05	0.87±0.05	0.88±0.05
$\gamma_{d,s}(D_s=1)$ #	1.56±0.05	1.16±0.05	1.08±.005
D†	0.91±0.1	0.51±0.1	0.46±0.1

+The divergence of moments exponents q_D are obtained from the wind field: $q_{D,}=q_{D,v}/3$.

The $\gamma_{d,s}(D_s)$ corresponds to the maximum observable dressed singularity for respective sampling dimensions (see Part I) D_s=0; 0.5; 1. The underlined values correspond roughly to values empirically accessible with the cited papers.

*This value is obtained by $K'(q_D)$.

† The dressing dimension D is obtained as solution of the implicit equation $K(q_D)= D(q_D\text{-}1)$

Table 2. Comparison of universal multifractal indices for *velocity* in the atmosphere in the vertical, horizontal and time.

Variable	Vertical (this paper)	Horizontal (part I)	Time (Schmitt et al., 1993)
α	1.85±.05	1.35±0.07	1.50±0.05
$C_{1,v}$ *	0.078±0.01	0.068±0.01	0.05±0.01
H	0.50±0.05	0.33±0.03	0.33±0.03
$q_{D,v}$**	5.0±0.02	7.0±1	7.0±1
$\gamma_{D,v}$	+0.06±0.03	-0.10±0.02	-0.10±0.03
$\gamma_{d,s,v}(D_s=0)$	-0.15±0.05	0.00±0.05	-0.04±0.05
$\gamma_{d,s,v}(D_s=0.5)$	-0.04±0.05	0.07±0.05	0.03±0.05
$\gamma_{d,s,v}(D_s=1)$	0.05±0.05	0.15±0.05	0.10±0.05
D_v†	0.33±0.1	0.22±0.1	0.20±0.1

*Calculated from $C_{1,v}=C_1 3^{-\alpha}$.

** $q_{D,v}= 3q_D$.

† The dressing dimension D_v is obtained as solution of the implicit equation: $K_v(q_{D,v})= D_v(q_{D,v}\text{-}1)$.

corresponding to a multifractal phase transition and to algebraic or "hyperbolic" fall-off of the probability distribution:

$$\Pr(X\geq x) \approx x^{-q_D}\ ;\ x>>1 \tag{7}$$

where the critical order of moment q_D (the analog of the reciprocal temperature of the critical phase transition) corresponds to the following divergence of statistical moments:

$$\langle x^q \rangle = \infty \quad q \geq q_D \tag{8}$$

The probability distribution function of wind shear $\Pr(\Delta V \geq \Delta v)$, plotted in Fig. 4 on log-log axes for different thresholds (Δv), exhibits nearly the same type of Self Organized Criticality (as pointed out by Schertzer and Lovejoy (1983, 1985) under the expression of "hyperbolic intermittency"), but over a wider range of intensities since our data set is much larger (ours involves $\approx 10^5$ measurements, theirs only $\approx 5\text{x}10^3$).

First, let us note that the uniform (left-right) separation (of factor $\approx 2^{H_v}$ since Δz is systematically increased by factors of 2) of the curves gives another estimate of H_v; the graph indicates the separation corresponding to the value $H_v \approx 0.51$. This is reasonably consistent with the theoretical value 3/5 , but is in good agreement with the estimate of H_v obtained in the next section.

For comparison, the straight lines corresponding to the best fit to the algebraic fall-off (for probability levels less then $10^{-2.5}$) are displayed on Fig. 4, leading us to an initial estimate $q_{D,v} \approx 5.0 \pm .2$. This is surprisingly close to the previous results (Schertzer and Lovejoy, 1983, 1985), who had found the similar slopes in the range of separations 50 m $\leq \Delta z \leq$ 3200 m with[9] $q_{D,v} \approx 5.0$, i.e. no preferred scale and convergence of moments only up to $\approx 5^{th}$ order.

5 The codimension of singularities $c(\gamma)$

We are naturally lead to compute the codimension function $c(\gamma)$, since it is the scaling exponent of the probability distribution (see Eq. 1 of part I) and therefore is obviously of more fundamental significance than the latter. As in Part I, we use a single scale implementation of the Probability Distribution Multiple Scaling (PDMS, Lavallée et al., 1991) technique which estimates $c(\gamma)$ as:

$$c(\gamma) \approx -\frac{\log \Pr}{\log \lambda} \tag{9}$$

i.e. it ignores a possible slowly varying prefactors of the probability in the definition of $c(\gamma)$.

From the plot of $c(\gamma)$ vs. γ, given on Fig. 5, we can once again obtain an estimate of H, as the tangent $c'(\gamma) = 1$ with the γ axis (this method exploits the fixed point of the $c(\gamma)$ function: $c(C_1\text{-}H)=C_1$ and $c'(C_1\text{-}H)=1$; see part I). This method yields an estimate of $H \approx 0.50$ which - given the method inaccuracy - is in good agreement with the value obtained from probability distributions 0.51 (see Sect. 4). From this curve we also obtain an estimate of C_1 which is the codimension of the mean process. We obtain a rough estimate $C_{1,v} \approx 0.1$. These values are larger than those obtained by Schmitt et al. (1992) for the temporal scaling of the wind at a point $C_{1,t} = 0.05 \pm 0.01$ and even larger than those obtained in the horizontal $C_{1,h} \approx 0.068 \pm 0.01$ in Part I.

[9]Other quanitties which were also found to display vertical scaling and divergence of moments were the potential temperature and gradient Richardson numbers.

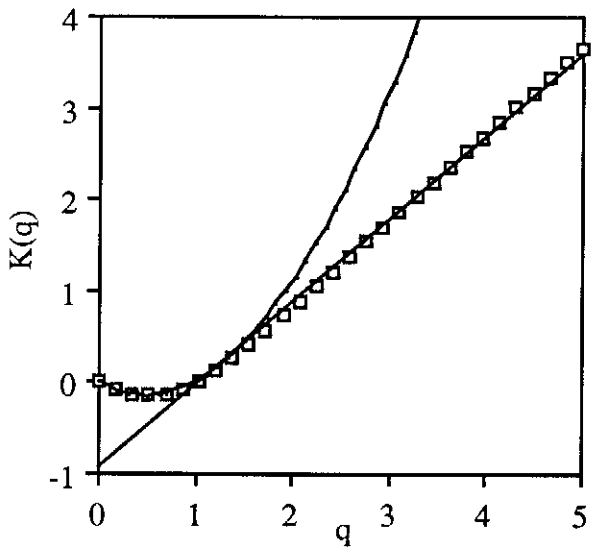

Fig. 7. The $K(q)$ curve calculated for a single realization showing with the theoretical bare curve (C_1=0.57, α=1.85), and the dressed curve for N_S=1, D_S=0 (hence $\gamma_{d,s}\approx$0.9, $q_s\approx$1.35). Since $q_s<q_D$ ($\approx$5/3), this is a second order multifractal phase transition.

Due to the space-time stratification, the various values of C_1 are not expected to be the same, see the discussion below. In the following section, $C_{1,v}$ will be more accurately determined using the Double Trace Moment technique. In the Fig. 5 we compare the empirical curve with that obtained using universal expressions for $c(\gamma)$, (see part I, Eq.(9)) with $C_{1,v}$=0.09, α=1.85, H_v=0.46, q_D=5 and $\gamma_D=K'(q_D)-H_v\approx 0.0$, showing the extremely good fit achieved. Note that the asymptotic linear behaviour of the dressed $c(\gamma)$ found here (associated with the first order multifractal phase transitions) is qualitatively different from the absolute maximum singularity postulated by the microcanonical models (e.g. Meneveau and Sreenivasan, 1987; Bershadskii and Tsinober, 1992; Bershadsky et al., 1993).

Another interesting point is that the critical order of singularity for the divergence of moments of the wind field ($\gamma_{D,v}$) is consistently close to the value 0, i.e. the corresponding velocity is nearly scale invariant. It is worth mentioning that this implies the possibility of observing positive order singularities (as displayed in Fig. 5). In the limit of infinite Reynolds number (i.e. $\lambda\rightarrow\infty$), $\gamma>0$ leads to infinite shears. Frisch 1991 postulated that this would be unphysical and used this restriction to justify his geometric (local) multifractal approach which has strongly bounded singularities and is generally not compatible with cascades (which involve nonlocal singularities). Schertzer et al 1994 criticized Frisch's argument on theoretical grounds[10], we see here that it also seems to be irrelevant on empirical grounds.

6 Universal multifractal indices determined by Double Trace Moment Analysis

The fundamentals of double trace moment (DTM) analysis were discussed in part I (Sect. 2). Here we rather focus on its application.

As in the horizontal case (Schmitt et al., 1992, 1993 and part I), we first must take into account the non conservation of shears (i.e. $H_v\neq 0$) as evidenced by the systematic left-right displacement of the probability distributions shown in Fig. 4. A statistically stationary series (necessary for the application of the DTM technique) can be obtained in various ways, the most appropriate here is by power law filtering in Fourier space, i.e. a fractional integration of order H_v. The main problem is that we are using wind velocity data while according to the Eq.(2) Bolgiano-Obukhov regime in the thermal convection is governed by the buoyancy force variance flux ϕ which is estimated via temperature data. So, first we have to get an accurate estimate of exponent H_v in the following scaling law for vertical wind shears:

$$\Delta v(\Delta z)\overset{d}{=}\left(\varepsilon(\Delta z)\right)^{a_v}\Delta z^{H_v} \qquad (10)$$

As was conjectured in Sect. 1, a balance between kinetic and thermal dissipation rates should be achieved when exponent a_v is equal to 1/3. And the estimate of H_v can be obtained using its meaning as the deviation from a conservative flux. So, a fractional integration of order H_v was done for different values until zero deviation was reached[11].

After fractional integration, samples were rased to the third power of the absolute value of the result was taken. This yields a conservative and positive quantity, which can be considered as an estimate of energy transfer rate ε. Each realization of ε obtained in this manner was used in the DTM analysis. The resulting functions $K(q,\eta)$ are shown on a log-log plot in Fig. 6. One can see that the curves are straight showing universal behavior over rather wide ranges of η and q values. The slope of the curves gives the value of the third parameter α (the Levy index of the generator), which we estimate as $\alpha_v=\alpha\approx 1.85\pm 0.01$.

Using the universal expression for $K(q,\eta)$ and this estimate of α, we can more precisely estimate the codimension of the mean process, respectively for the energy and shears, as: $C_1\approx 0.59\pm 0.05$, $C_{1,v}\approx 0.078\pm 0.01$. Finally, Fig. 7 shows the comparison of the empirical K(q)

[10]Indeed, in incompressible Navier-Stokes turbulence, the speed of sound is infinite and in the infinite Reynolds limit there is no convincing reason that the velocities shears remain finite. Furthermore, even with a compressible fluid and finite Reynolds number, positive singularities can exist without leading to velocities exceeding the speed of sound (in the atmosphere $\gamma\approx$0.2 are still compatible with this limit). Finally, the velocity of sound is not an absolute bound anyhow.

[11]At the value $H_v\approx$0.5 which due this fundamental property seems to be the most reliable estimate for H_v (inspite of the above discussions on H_v values).

function for a single realization, compared with the theoretical curve obtained with the observed C_1, α and with $q_s=c'(\gamma_s)$ and $c(\gamma_s)=1$. This shows that only 2nd order phase transitions occur on single realizations.

7 Discussion

We can now compare our results with those obtained earlier in time (Schmitt et al., 1993), and the horizontal (part I), this is shown in Tables 1, and 2, the underlined values of the maximum observable (dressed) singularity corresponds roughly to the sizes of the data bases used for the estimates.

In the Tables we have shown the values of $\gamma_{d,s}$ corresponding to a single sample ($D_s=0$) and increasing sample size (calculated from $c_d(\gamma_{d,s})=D+D_s$. D is the dimension of the observing space = 1 in all these cases, (i.e. time, aircraft or balloon trajectory). $D_s = Log(N_s) / Log(\lambda)$ is the sampling dimension, and N_s is the number of samples. Note that for single samples, the divergence cannot be detected in the vertical ($\gamma_{d,s} < \gamma_D$) and it is marginally detectable in the horizontal and in time ($\gamma_{d,s} \approx \gamma_D$).

We have already noted that the H values are close to those predicted by dimensional arguments. This result already lead to a simple model of the atmosphere involving an overall stratification characterized by a single linear generator G with trace = the elliptical dimension = $2+H_z$ with $H_z=H_h/H_v=5/9$ (Schertzer and Lovejoy 1983, 1985). This simplest model predicts that both weak and mean events will have codimensions which are in the same ratio:

$$\frac{C_{1,h}}{C_{1,v}} = \frac{H_h}{H_v} = H_z = \frac{5}{9} \tag{11}$$

empirically, we find for ε the ratio $C_{1,h}/C_{1,v}$ = 0.3/0.59 =0.51 which is rather close to the predicted value 0.555. This agreement indicates that at least for low order statistics the original scalar model based on deterministic linear generalized scale invariance works remarkably well.

However, the fact that the values of α in the horizontal and vertical are close but distinct, although they both belong to the same class of unconditionally hard universal multifractals ($\alpha>1$), implies that it cannot hold exactly for higher intensity levels, since they will be more sensitive to the different type of distribution of singularities ruled by the index of multifractality α. This points out that the original model should be improved by searching a more complex (e.g. vectorial) balance between the horizontal shears and vertical buoyancy forces, which in the original model was simply expressed by the scalar balance (see Eq.3 between their respective scalar fluxes. This requires an explicit treatment of the vector nature of the problem using Lie cascades (Schertzer and Lovejoy 1994).

8 Conclusions

In the second part, we have first confirmed previous multifractal analyses along the vertical but in the tropics rather than midlatitudes, and using a much larger data base. Other differences include the use of more sophisticated analysis methods (especially the Probability Distribution Multiple Scaling and Double Trace Moment techniques). The combination of these radiosonde results with the aircraft analyses discussed in part I, performed on data collected in the same area and period, gave us the unique opportunity to test the unified multifractal model of atmospheric dynamics with data with essentially the same meteorological and climatological characteristics.

Using a single generator of anisotropy, our model unifies the small and large scale horizontal and vertical structures by a single anisotropic scaling regime rather than two separate isotropic 2D and 3D regimes. It also unifies the weak and the strong fluctuations by using a single probability generator characterized by three basic (universal) multifractal parameters which we estimate. For intensities near the mean, we reconfirm that the monofractal exponent H (characterizing the deviation of the velocities from the conserved energy and buoyancy fluxes) are close to the theoretical values obtained by dimensional arguments: H_h = 1/3, H_v= 3/5. Empirically, we find that the other monofractal exponent C_1 (characterizing the sparseness of the mean) is transformed from the horizontal to the vertical using the anisotropy implied by the different H values: $C_{1,h} = H_v\, C_{1,v} / H_h$. The original unified scaling model is therefore adequate for singularities, not too far from the mean (i.e. for not too extreme events), this is apparently true in both the tropics as well as the mid latitudes.

However, using the Double Trace Moment technique, we obtained convincing results showing that the multifractal index α was not the same for the vertical and horizontal directions (and apparently different from that in time) and as a consequence we obtain somewhat different behaviours for the extreme fluctuations (associated with Self Organized Critical structures) along the vertical when compared to the horizontal. In order to account for this effect, we must go beyond the original scalar framework in order to better take into account the fundamental balance between shears and buoyancy forces.

Acknowledgments. We are particularly indebted for many stimulating discussions with F. Schmitt. Part of this research was supported by contract EEC # FI3P-CT930077, and grant RFFI 94-01-01241-a.

References

Adelfang, S. I., On the relation between wind shears over various intervals, *J.Atmos. Sci., 10*, 138, 1971.

Bershadskii, A., Kit, P, Tsinober, A., Vaisburd, H., Intermediate multifractal asymptotics and strongly localized events of energy, dissipation, enstrophy and entropy generation. *IMA Conference on Multiscale Stochastic Processes Analysed using Multifractals and Wavelets*. Cambridge, 29-31 March, 1993.

Bershadskii, A., Tsinober, A., Asymptotic fractal and multifractal properties of turbulent dissipative fields. *Physics letters, A, 165*, 37, 1992.

Bolgiano, R., Turbulent spectra in a stably stratified atmosphere, *J. Geophys. Res., 64*, 2226, 1959.

Brandenberg, A., Energy spectra in a model for convective turbulence, *Phys. Rev. Lett., 69*, 605, 1992.

Chiriginskaya Y., Schertzer, D., Lovejoy,S., Lazarev, A., Unified Multifractal atmospheric dynamics tested in the tropics: part I, horizontal scaling and Self Organized Criticality, *Nonlinear Processes in Geophysics*, 1994, (this volume).

Daniels, G., Terrestrial environment (climatic) criteria guidelines for use in aerospace vehicle development, *1982 Revision, NASA Tech. Memo*, NASA-TM-84273, 1982.

Endlich, R.M., Singleton, R.C. and Kaufman, J.W., Spectral analysis of detailed wind speed profiles, *J. Atmos. Sci., 26*, 1030-1041, 1969.

Frisch, U., From global scaling à la Kolmogorov, to local multifractal scaling in fully developed turbulence. *Proc. Roy. Soc. Lond. A, 434*, 89-99, 1991.

Kolmogorov, A. N., Local structure of turbulence in an incompressible liquid for very large Reynolds numbers. *Proc. Acd. Sci. URSS, Geochem. Sect. 30*, 299-303, 1941.

Lavallée, D., Lovejoy, S., Schertzer, D., On the determination of universal mulifractal parameters in turbulence. *Nonlinear Variability in Geophysics: Scaling and Fractals*. Kluwer, eds D. Schertzer and S. Lovejoy, 99-110, 1991.

Lavallée, D., Lovejoy, S., Schertzer, D., Schmitt, F., On the determination of universal multifractal parameters in turbulence. *Topological aspects of the dynamics of fluids and plasmas*, Eds. K. Moffat, M. Tabor, G. Zaslavsky, 463-478, Kluwer, 1992.

Lilly, D.K., Mesoscale varaibility of the atmosphere. *Mesoscale Meteorlogy -Therories , Observations and Models*, eds D.K. Lilly and T. Gal-Chen, D. Reidel, 13-24, 1983.

Lovejoy S. , Schertzer, D., Silas, P., Tessier, Y., and Lavallée, D., The unified scaling model of atmospheric dynamics and sytematic analysis of scale invariance in clouds radiances. *Ann. Geophysicae, 11*, 119-127, 1993.

Meneveau, C. and Sreenivasan, K.R., Simple multifractal cascade model for fully develop turbulence. *Phys. Rev. Lett. 59*, 13, 1424-1427, 1987.

Myrup, L.O., Turbulence spectra in stable and convective layers in the free atmosphere, *Tellus, 21*, 341-354, 1969.

Nastrom, G.D. and Gage, K.S., A first look at wave number spectra from GASP, *Tellus, 35*, 383, 1983.

Obukhov, A.N., On the distribution of energy in the spectrum of turbulent flow, *Sov. Phys. Dokl., 32*, 57-66, 1941.

Obukhov, A.N., Effect of Archimedian forces on the structure of the temperature field in a temperature flow, *Sov. Phys. Dokl., 125*, 1246, 1959.

Pinus, N.Z., Reiter, E. R., Shur, G.N., and Vinnichenko, N.K., Power spectra of turbulence in the free atmosphere, *Tellus, 19*, 206, 1967.

Rosenberg, N.W., Good, R.E., Vickery, W.K., and Dewan, E.M., Experimental investigation of small scaler transport mechanisms in the stratosphere, *AIAA J., 12*, 1094-1099, 1974.

Schertzer, D., Lovejoy, S., Elliptical turbulence in the atmosphere. *Proceedings of the 4th symposium on turbulent shear flows*, 11.1-11.8, Karlsrhue, West Germany, 1983.

Schertzer, D. and Lovejoy, S., The dimension and intermittency of atmospheric dynamics, *Turbulent Shear Flows 4*, 7-33, ed. B.Launder et al., Springer, NY, 1985.

Schertzer, D. and Lovejoy, S., Hard and soft multifractal processes, *Physica A., 185*, 187-194, 1992.

Schertzer, D., Lovejoy, S., From scalar to Lie cascades: joint multifractal analysis of rain and clouds porcesses.. *Space/Time Variability and Interdependence of Hydological Processes*, R.A. Feddes ed., Cambridge University Press, 1994 (in press).

Schertzer, D., Schmitt, F., Lovejoy, S., On an erroneous turbulence theorem. *Ann. Geophysicae, 12 , II*, C 510, 1994.

Schmitt, F., Schertzer, D., Lovejoy, S., Brunet, Y., Estimation of universal multifractal indices for atmospheric turbulent velocity fields. *Fractals, 1*, 568-575, 1993a.

Schmitt, F., Schertzer, D., Brethenoux, G., Lovejoy, S., and Brunet, Y., Transition de phase multifractale du premier ordre en turbulence atmosphérique. *Cr. Acad. Sci. Paris*, 1993b (submitted).

Vinnichenko, N.K. and Dutton, J.A., Empirical studies of atmospheric structure and spectra in the free atmosphere, *Radio Sci., 4*, 1115, 1969.

Yakhot, V., 4/5 Kolmogorov law for statistically stationary turbulence: application to high Rayleigh number Benard convection, *Phys. Rev. Lett., 69*, 769, 1992.